Available online www.jocpr.com

Journal of Chemical and Pharmaceutical Research, 2014, 6(2):660-667

Research Article

ISSN : 0975-7384
CODEN(USA) : JCPRC5

Medical clinical ultrasound image segmentation based on modified wavelet transformation method

Xiaojun Wang* and Weidong Lai

Science & Technology College, North China Electric Power University, Baoding, Hebei Province, P. R. China

---

ABSTRACT

Ultrasound medical image has drawn extensive attentions for clinical monitoring and pharmaceutics determination, and the quality of image plays essential role for accurate information interpretation. In order to improve the contrast of the ultrasound medical image, algorithm based on modified wavelet transformation method has been established and optimized in this article. The modules maximum criterion is proposed for segmenting edges from the blurring background, though many pseudo-edges appear. Definition on the continuous of the edge according to the amount as P of the connected pixels implies that the higher coefficient P has induced the preservation of longer edges, and shorter segmented edges with fewer pixels have been erased. Entropy calculation indicates that the lower P has arisen out more decrease entropy deviation, and optimal threshold of P coefficient is defined at the 10% entropy deviation from the original ultrasound image. Consequently, the ultrasound image has been segmented out with more essential edges by the combined criterions of modules maximum, edge continuous and optimal entropy. The obtained algorithm can be integrated into the clinical evaluation software for ultrasound image interpretation to enhance the diagnostics and pharmacology accuracy.

Keywords: Ultrasound medical image, wavelet transformation, maximum modulus, entropy threshold, pharmacology accuracy

---

INTRODUCTION

Information detection and recognition on the human being body plays important roles in clinical pathology and pharmacology [1], which can not only be obtained through the sample reports such as auscultation, palpation and thermometric analysis, but also by the multi-modal images derived from X-rays, CT (Computerized Tomography), MR (Magnetic Resonance), US (Ultrasound) and so on [2-3]. Since the inner structure of the body can be revealed without severe damages, the medical images have been accepted as the major diagnostics supports in modern clinical activity [4]. For all kinds of medical images, there have the same inherent technical characteristic as the untouched energy ray scanning for image acquisition, though the ray wavelength is different for detecting different body structures. For example, the X-Ray can be utilized to detect the skeleton, MR to display the parenchyma, and the US responding to the viscus [5]. Though all medical images have unique meaning for acquiring the pathological change information, the ultrasound technique can be widely generalized at low cost, especially in the developing countries. Ultrasound approach has been increasingly used as first aid response for emergency cases [6].

Due to the complex composition of human body organs and air bubble environments, the ultrasound images are inevitably deteriorated by noises derived from different sources to generate the echo texture, speckle, weak edges and so on [7-8]. In order to heighten the diagnosis accuracy, many algorithms have been investigated and practiced. *Mateo* et al. review the general filters for speckle noise reduction in the ultrasound images, including median filter, adaptive weighted median filter, *Fourier* filter as well as wavelet filter. It presents that the best quality images are obtained with *Fourier* filter, and the others only provide some definite degree of improvement [9]. *Chen* et al. report two algorithms, one as the discrete region competition and the other of the weak edge enhancement, with the

proposed new approaches been implemented and verified on clinical ultrasound images [10]. *Kurnaz* et al. obtain an incremental neural network (INeN) for the segmentation of tissues in ultrasound images. Compared to the *Kohonen* network (KN), INeN automatically produces a topology according to the patterns in the input feature space, and achieves segmentation of the ultrasound images without any expert experience [11].

From morphology viewpoint, the ultrasound image is constructed by pixels with varied gray levels. The edge of image is obviously formed by continuous pixels, with the noise points usually as discrete variability pixels. Image morphological segmentation is important to partition the image into regions with medical meanings [12].

In this article, the modified wavelet transform algorithm is proposed by judging the validity of the segmented edges, and extracting the ultrasound information from noise background. The proposed algorithm can be integrated into expert system for ultrasound information analyzing. This article is organized as follows. Section 2 presents a basis of the wavelet algorithm. The modified wavelet transformation is proposed in Section 3, with the ultrasound image segmentation effect displayed and evaluated. The last section concludes this article.

2. Wavelet algorithm application in medical image transformation

Representations of multi-resolution image based on wavelet transformation have become very important, owing to their effectiveness to capture image features that occur at different frequency scales.

The wavelet transformation is defined as the convolution between the original signal $f(t)$ and the wavelets as [13]

$$Wf(a,b) = \frac{1}{a}\int_{-\infty}^{+\infty} f(t)\varphi(\frac{b-t}{a})dt \quad \textbf{(1)}$$

In which, the $\varphi((b-t)/a)$ is the wavelet arrays after dilating and shifting the core function $\varphi(t)$ by the spatial constants of a and b. Wf is the wavelet-transformed coefficients. The wavelet $\varphi(t)$ has the properties that its amplitude is started at zero, then increased, and finally decreased back to zero, with the total integral of zero.

The wavelet transformation has been introduced for processing two-dimensional (2D) medical images.

For the 2D digital medical image, the discrete wavelet transform (DWT) [14] is applied to decompose the image into superposition of wavelets, and the transformed coefficients can be displayed as Fig. 1.

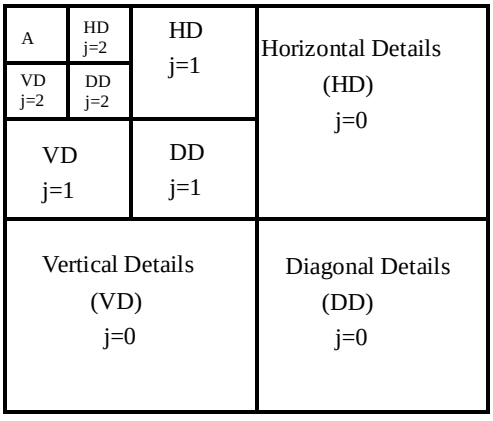

Fig. 1 Wavelet decomposed structures at different levels for 2D medical image

These coefficients are arranged in different j^{th} resolution levels, which can be considered as the operation of low-pass and high-pass filters on the original image [15]. The approximate information in low frequency scale and the detail information in the high frequency scale of the image have been obtained.

Overall, the wavelet core function $\varphi(t)$ is important for such 2D convolution wavelet decomposition.

RESULTS AND DISCUSSION

In this article, the 22-weeks embryo in uterus is scanned by ultrasound, as shown in Fig. 2. Such ultrasound-based medical image has widely been applied to monitor the internal tissues in uterus, in order to capture their size,

structure and any pathological lesions for low risk pregnancies. Since the image is sourced from the reflected ultrasound signal, extra noise signal would also be scanned. In Fig. 2, gray speckles have distributed in the whole image. Such a phenomenon is universal, and should be ascribed to the noise or defect from ultrasound instrument or the air bubble environment in uterus.

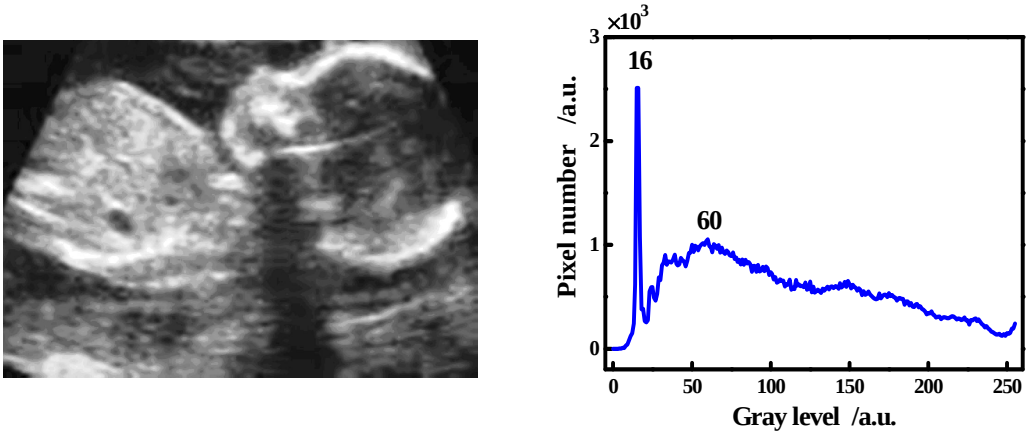

(a) **(b)**

Fig. 2 (a) US image of the embryo in uterus, and (b) its corresponding pixel gray level distribution

The selected US image is quantitatively evaluated by the pixel gray level distribution in Fig. 2b. The highest peak at gray level of 16 is discretely appeared from the continuous distribution profile with peak at gray level of 60. Major part of the pixels is black and gray in color. And it is obvious that the most important information of the US image is embedded in the edges.

In this paper, the modified wavelet algorithm is designed and utilized to segment the image for acquiring the clinical meaning edges.

3.1 Wavelet function definition and transformation

The wavelet $\varphi(x, y)$ is defined through the first order differential operation on certain core function $\Phi(x, y)$, and shown as follows.

$$\varphi_1(x,y) = \frac{\partial \phi(x,y)}{\partial x}$$
$$\varphi_2(x,y) = \frac{\partial \phi(x,y)}{\partial y} \quad \textbf{(2)}$$

Such core $\Phi(x, y)$ in Eq.(2) is set as the two-dimensional smooth *Gauss* function in

$$\phi(x,y) = \frac{1}{\sqrt{2\pi}} \exp(-\frac{x^2+y^2}{8}) \quad \textbf{(3)}$$

For the two-dimensional medical image, its pixel coordinated at (x, y) is present as matrix element $f(x, y)$, with f of the gray level intensity. Then wavelet transform is applied in two directions through convoluting the $f(x, y)$ by the respective normalized wavelet $\varphi(x, y)$ in its matrix form as follows.

$$W_1[f(x,y)] = f(x,y) * \varphi_1(x,y)$$
$$W_2[f(x,y)] = f(x,y) * \varphi_2(x,y) \quad \textbf{(4)}$$

Consequently, the two-dimensional wavelet transformation coefficients have been obtained, which are proportional to the gradient value of $f(x, y)$ at respective x and y direction in mathematical meanings. Such coefficients are imaged in Fig. 3. There have the horizontal and vertical features respectively extracted from the original images. But the image edges are too faint to discriminate out the clinical information.

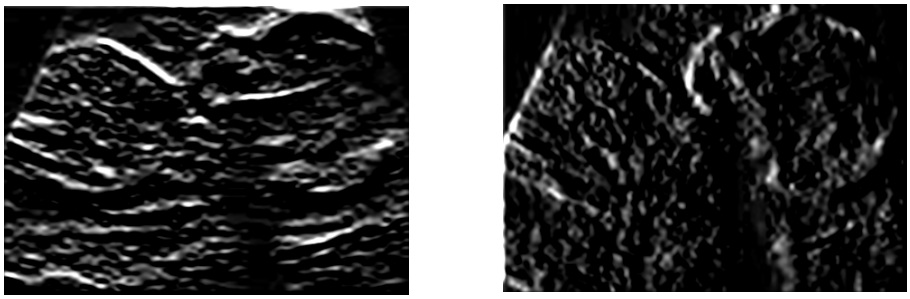

(a) (b)

Fig. 3 The two-dimensional presentation of (a) W_1 coefficients and (b) W_2 coefficients

3.2 Maximum modulus operation on the transformed coefficients

In order to enhance the image edges, the modulus M of the wavelet transformation coefficients $W[f(x, y)]$ is defined in Eq.(5), and is proportionally related to the magnitude of gradient. The phase angle of such gradient vector is also computed from the inverse tangent between the ratio of $W_2[f(x,y)]$ and $W_1[f(x, y)]$ in Eq.(6).

$$M = \sqrt{W_1[f(x,y)]^2 + W_2[f(x,y)]^2} \quad \textbf{(5)}$$

$$\theta = \arctan \frac{W_2[f(x,y)]}{W_1[f(x,y)]} \quad \textbf{(6)}$$

In general, edge pixel of an image is corresponding to rapid variance of gradient in its neighborhood scale. Edge pixels in the medical image are detected according to maximum modulus criterion along the respective phase angle directions, just as follows.

Criterion 1 Pixel $f(x_0, y_0)$ is on the image edge, only if $|M[f(x, y)]|<|M[f(x_0, y_0)]|$ in the neighborhood of $f(x_0, y_0)$ at given phase angle direction.

The wavelet transformed modules are calculated according to Eq.(5) and shown in Fig. 4a. There have pseudo-edges appeared. To judge out the wavelet coefficients related to the image edges, the maximum modulus at given phase angle directions has been obtained after traversing the whole modulus matrix. Result is shown in Fig. 4b.

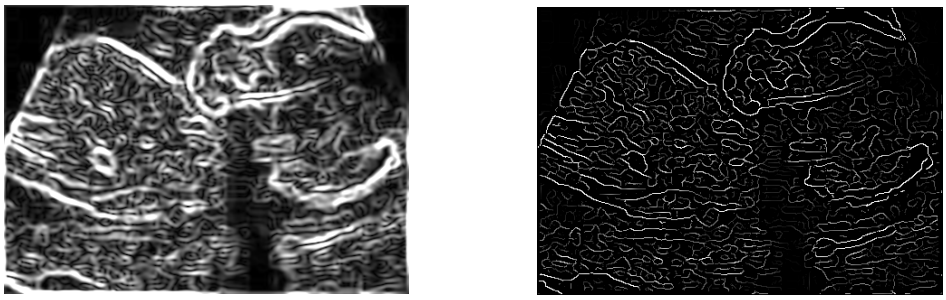

(a) (b)

Fig. 4 (a) Modulus image. (b)Maximum modulus treated Fig.4a according to Criterion 1

After maximum modulus criterion operated, some pseudo-edges have been attenuated, and the embryo profile as well as most of the details in the body has been preserved.

To enhance the original image, the maximum modulus manipulated image of Fig. 4b is segmented onto the original one as red color edges to generate the Fig. 5. The edge structure of the embryo has been distinctly specified, and high contrast is achieved between the microstructure and the artificially enhanced edges. But it should be noticed that there have too many edges to disturb the image comprehension.

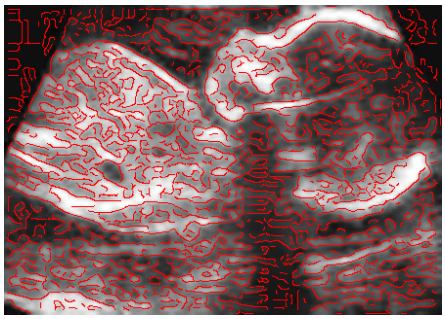

Fig. 5 US image segmented by red-color edges selected from the maximum modulus criterion

3.3 Edge discrimination based on the threshold of continuous pixels and entropy

Due to the too many edges, the US image in Fig. 5 has more textures to deteriorate the clinical accuracy. In order to discriminate out the important edges, the judge criterion is defined as follows.

Criterion 2 Important edge possesses continuous pixels, only if the pixel amount is larger than P, in which P is a number lower than the image size.

The neighborhood traversing algorithm is established to removes all edges in the segmented image that have pixels with the amount fewer than P.

Different results have been obtained in Fig. 6. There has a contradiction that more edges can enhance the local contrast and deteriorate the whole image quality. In Fig. 6a, when the continuous criterion on edge is set at P of 10, many edges have segmented the image, but too more microstructures have also been outlined. The higher the P is, the longer the edges have been preserved. And shorter edges with few pixels have been erased.

In Fig. 6f, only embryo outer profile is approximated and much edge information disappears when the P is 150. There should establish some method to evaluate the segmentation effect on the US image.

To do this, the segmented edges are converted into white color with the pixel gray level of 255, and exampled in Fig. 7 for the images processed at P=10 and 70. The texture in the segmented images is statistically measured by entropy, which is defined as

$$E = -\sum_{i=0}^{255} p_i \log(p_i) \tag{7}$$

In which, p_i is the probability of the pixels with gray level of i in the $m \times n$ sized image as

$$p_i = \frac{\sum_{x,y}^{m,n} (f(x,y) == i)}{m \times n} \tag{8}$$

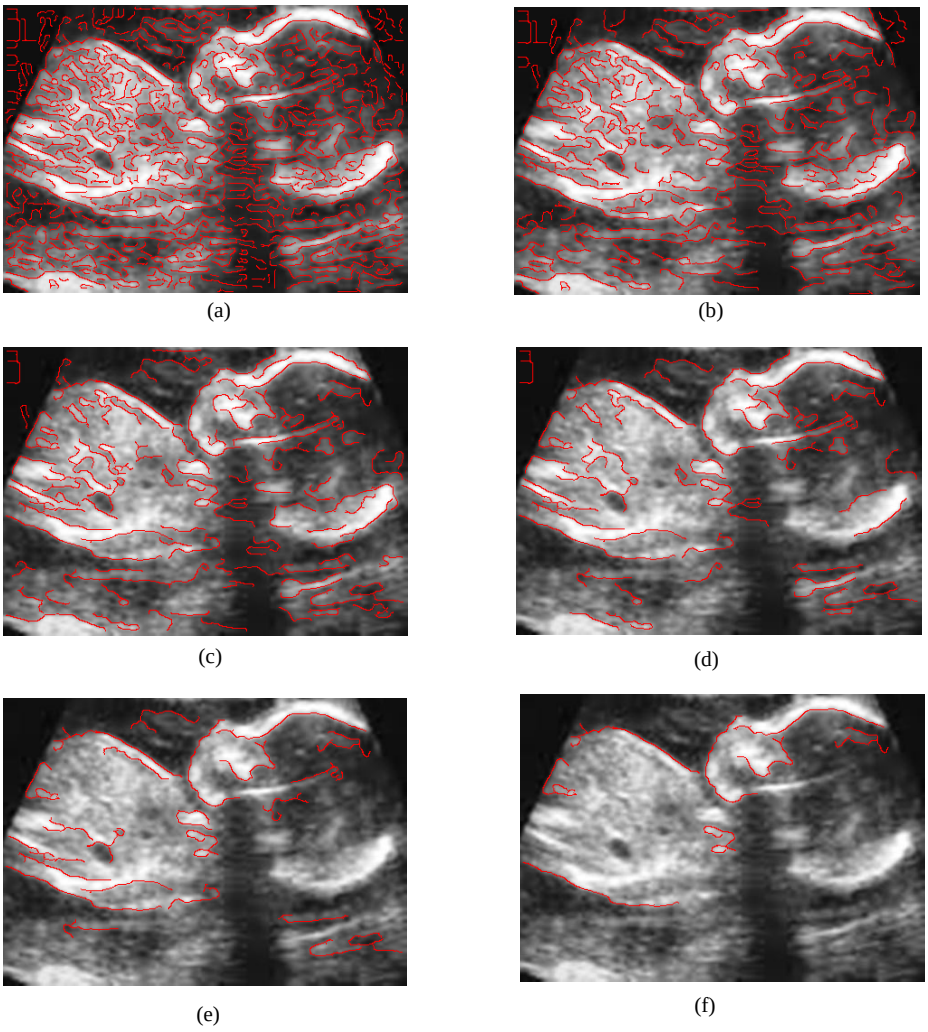

Fig. 6 US image segmented by red-color edges selected by the Criterion 1 and 2 with the pixel amount set as P (a) P=10; (b) P=30; (c) P=50; (d) P=70; (e) P=100; (f) P=150

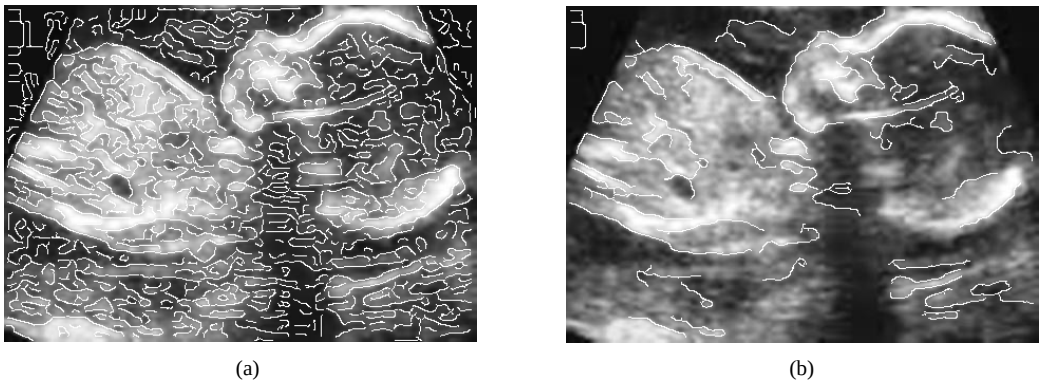

Fig. 7 US image segmented by white color edge selected by the Criterion 1and 2 with the pixel number threshold set as P. (a) P=10; (b) P=70

The entropy of Fig. 7a is calculated as 7.28729, and that in Fig. 7b is 7.68768. The higher P has induced larger entropy. Such a phenomenon is ascribed that too more short edges have enlarged the probability of pixels at gray level of 255, but the whole entropy is weakened due to the decreased probability of the pixels substituted by the short edges. Contrarily, when only the longer edges are discriminated out from the edge arrays, the pixel distributions in the segmented microstructures are not remarkably influenced as shown in Fig. 7b, and the entropy is increased.

The entropy is calculated at different P value, and present in Fig. 8. A monotonically increasing trend appears. When the edges are evaluated by too higher P value, the image without segmentation effect has been regenerated since there have no such longer edges. And the entropy is nearly constant at higher P values.

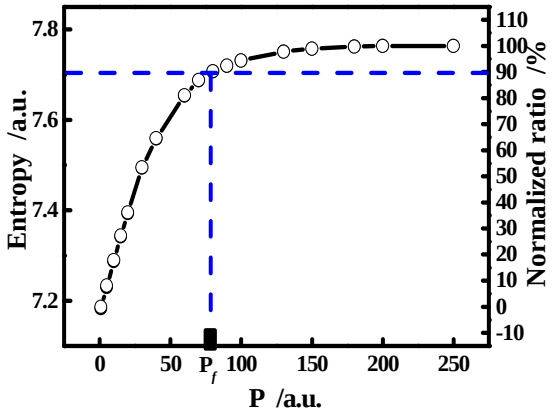

Fig. 8 Entropy variance of the segmented ultrasound image versus the P value

Then the judge criterion on favorite segmented image is defined as follows.

Criterion 3 The favorite segmented image is at the optimal P_f, only if the P_f value is corresponding to the image with 10% entropy deviation from the original image.

Consequently, the optimal P_f is calculated as 79 by processing the entropy variance curve. At such a selected value, the segmented ultrasound image is present. The whole profile of the embryo image has been outlined in Fig. 9a, and the main structures in the body are discriminated out without too many minor microstructures circled. There has some degree of improvement achieved.

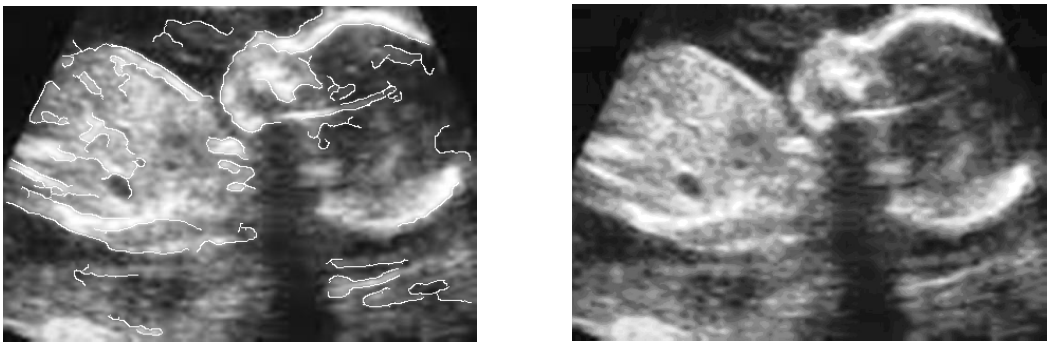

(a) (b)

Fig. 9 (a) The segmented ultrasound image processed at the optimal P value of 79, and (b) the original ultrasound image putted as reference

CONCLUSION

Ultrasound image has been widely utilized for clinical diagnosis at low cost. Due to the body bubble environment and the low energy of the ultrasound, there have noise deteriorated the clinical accuracy of the image. The modified wavelet transformation method based on maximum modulus judgment is proposed to segment the medical image in order to heighten its contrast. But too many pseudo-edges have disturbed the interpretation on the segmented image. Then two criterions are emphasized on remediating the disturbance. One is the longer edge discrimination based on the edge continuous property. The other is the definition about the optimal continuous coefficient based on the image entropy. Results indicate that the higher coefficient P, which is corresponding to the pixel number threshold in a continuous edge, has induced the preservation of longer edges, and shorter segmented edges with little pixels have been erased. In order to evaluate the segment effect at different P coefficients, the entropy of the segmented image is calculated. It finds that the lower the P is, the higher the deviation becomes between the segmented image and the original one. The optimal image is defined at the P coefficient corresponding to 10% entropy deviation. Ultrasound image with more essential edges have been optimally segmented out.

The combined algorithm can be directly integrated into the clinical evaluation software for ultrasound image interpretation to enhance the accuracy of diagnostics and pharmacology.

Acknowledgments
This work is financially supported by the Fundamental Research Funds for the Central Universities No. 12MS146.

REFERENCES

[1] JS Duncan; N Ayache. *IEEE T. Pattern Anal.*, **2000**, 22(1), 85-106.
[2] F Luo; BB Lu; CL Miao. *J. Chem. Pharm. Res.*, **2013**, 5(12), 215-220.
[3] XW Li. *J. Chem. Pharm. Res.*, **2013**, 5(12), 113-117.
[4] R Tadeusiewicz; MR Ogiela. *Medical image understanding technology*, Springer, Berlin-Heidelberg, **2004**; 7-78.
[5] JJ Zhao; YX Liu; MY Qu; Y Qiang. *J. Chem. Pharm. Res.*, **2013**, 5(12), 188-195.
[6] JA Noble. *P. I. Mech. Eng. H*, **2010**, 224(2), 307-316.
[7] H Rabbani; M Vafadust; P Abolmaesumi; S Gazor. *IEEE T. Bio-Med. Eng.*, **2008**, 55(9), 2152-2160.
[8] N Damodaran; S Ramamurthy; S Velusamy; GK Manickam. *Ultrasound Med. Biol.*, **2012**, 38(2), 276-286.
[9] JL Mateo; A Fernández-Caballero. *Expert Syst. Appl*., **2009**, 36(4), 7786-7797.
[10] CM Chen; H Horng-Shing Lu; YL Chen. *Pattern Recogn. Lett.*, **2003**, 24(4), 693-704.
[11] MN Kurnaz; Z Dokur; T Ölmez. *Comput. Meth. Prog. Bio.*, **2007**, 85(3), 187-195.
[12] MC Moraes; SS Furuie. *Ultrasound Med. Biol.*, **2011**, 37(9), 1486-1499.
[13] YS Xu; JB Weaver; DM Healy Jr; J Lu. *IEEE T. Image Process.*, **1994**, 3(6), 747-758.
[14] Y Yang; DS Park; SY Huang; NN Rao. *EURASIP J Adv. Sig. Pr.*, **2010**, 579341.
[15] H Li; BS Manjunath; SK Mitra. *Graphical Models and Image Processing*, **1995**, 57(3), 235-245.